High-Efficiency Loading and Controlled Release of Doxorubicin Hydrochloride on Graphene Oxide

Xiaoying Yang,*,† Xiaoyan Zhang,‡ Zunfeng Liu,‡ Yanfeng Ma,‡ Yi Huang,‡ and Yongsheng Chen*,‡

School of Pharmaceutical Sciences, Tianjin Medical University, Tianjin 300070, China, Center for Nanoscale Science and Technology and Key Laboratory of Functional Polymer Materials, Institute of Polymer Chemistry, College of Chemistry, Nankai University, Tianjin 300071, China

Received: July 30, 2008; Revised Manuscript Received: September 10, 2008

A novel graphene oxide−doxorubicin hydrochloride nanohybrid (GO−DXR) was prepared via a simple noncovalent method, and the loading and release behaviors of DXR on GO were investigated. An efficient loading of DXR on GO as high as 2.35 mg/mg was obtained at the initial DXR concentration of 0.47 mg/mL. The loading and release of DXR on GO showed strong pH dependence, which may be due to the hydrogen-bonding interaction between GO and DXR. The fluorescent spectrum and electrochemical results indicate that strong $\pi-\pi$ stacking interaction exists between them.

1. Introduction

Nanoscaled drug carriers have emerged as a bridge linking nanotechnology and advanced drug delivery, involving nanoscaled materials such as liposomes,[1] microspheres,[2] polymeric shells,[3] nanoparticles,[4] carbon nanotubes,[5] and carbon nanohorns.[6] The medicine is loaded on these nanoscaled materials by many kinds of mechanisms, such as embedding, surface absorption, hydrogen bonding, and other types of interactions, while the loading capacity of the current developed nanoscaled drug carriers toward the drugs is still low, normally less than 100%. Therefore, for efficient drug action, improving the loading efficiency is critical in drug carrier research. Recently, Dai et al.[7] described the ultrahigh loading capacity of highly aromatic molecules toward carbon nanotubes via strong π-stacking interactions. Graphene, as a very recent rising star in material science with two-dimensional structure consisting of sp^2-hybridized carbon, like carbon nanotubes, exhibits remarkable electronic and mechanical properties.[8,9] Its one-atom thickness and large two-dimensional plane provide it large specific surface area. However, little has been done to explore graphene in biological systems. Dai et al.[10,11] reported PEG-ylated nanographene oxide for delivery of water-insoluble cancer drugs and found that the functionalized nanographene sheets are biocompatible without obvious toxicity and can be loaded with aromatic anticancer drug with high efficiency. While carbon nanotubes and nanohorns load drugs mainly via surface and tips and form serious bundles when used as drug carrier materials, the graphene sheet is expected to load drugs via its two faces and edges. After oxidation, the graphene can be introduced with hydrophilic groups such as hydroxyl and carboxylic and can be well-dispersed in aqueous solution,[12] which makes it a promising material as a drug carrier substance.

Herein, we report a novel noncovalent nanohybrid formed by GO with DXR and investigate the in vitro binding and release of DXR by GO. The amount of DXR loaded onto GO is significantly high and dependent on pH value. Furthermore, the interaction between DXR and graphene was investigated by spectroscopy and electrochemistry.

2. Experimental Section

Apparatus and Chemicals. Fourier transform infrared spectrometer (FT-IR) (Tensor 27, Bruker), ultraviolet−visible−near IR spectrophotometer (UV−vis−NIR) (JASCO, V-570), atomic force microscope (AFM, Nanoscope IV, Digital Instruments, Veeco) and spectrofluorometer (Jobin Yvon, FluoroMax-P) were used to characterize the GO−DXR nanohybrid. Electrochemical experiments were performed with a microcomputer-based electrochemical analyzer (Lanlike, LK98B).

Graphite was purchased from Qingdao Tianhe Graphite Co. Ltd.,with an average particle diameter of 4 μm (99.95% purity). Doxorubicin hydrochloride (DXR) was purchased from Beijing Huafeng United Technology Co. Ltd. a dialysis chamber for the drug release was purchased from Beijing Dingguo Biotechnology Co. (diameter =36 mm), which had a molecular weight cutoff of 8000−15 000 g/mol.

Preparation of Water-Soluble, Individual Graphene Oxide. Graphene oxide (GO) was prepared from purified natural graphite according to a modified Hummer's method.[12]

Conjugation of DXR and GO. GO with the final concentration of 0.145 mg/mL (determined using a standard GO concentration curve at the absorption of 230 nm) was first sonicated with DXR with a certain concentration at a certain pH value for 0.5 h and then stirred overnight at room temperature in the dark. All samples were adjusted to pH <6 with 1 M hydrochloride and then ultracentrifuged at 14 000 rpm for 1 h.

Characterization of GO−DXR. The amount of DXR loaded on GO was determined as follow. The DXR concentration in the upper layer was measured using a standard DXR concentration curve generated using the UV−vis spectrophotometer from a series of DXR solutions with different concentrations. The

* Corresponding authors. Phone: +86 (22) 2350-0693. Fax: +86 (22) 2349-9992. E-mail: yangxiaoying@tijmu.edu.cn (X.Y.), yschen99@nankai.edu.cn (Y.C.),

† Tianjin Medical University.

‡ Nankai University.

10.1021/jp806751k CCC: $40.75
Published on Web 10/21/2008

SCHEME 1: Structures of GO and DXR

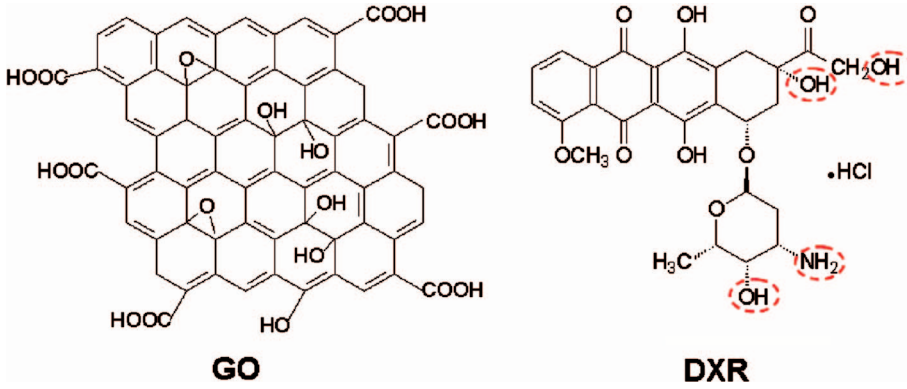

DXR concentrations were measured at the wavelength of 233 nm. The amount of DXR loaded on GO was determined using eq 1

$$\Phi = (M_{DXR} - M_{DXR}')/M_{GO} \quad (1)$$

where Φ is the amount of DXR loaded on GO, M_{DXR} is the initial amount of DXR, M_{DXR}' is the amount of DXR in the upper layer, and M_{GO} is the amount of GO added.

The resultant products of GO−DXR were characterized by UV−vis spectrophotometer, FT-IR spectrometer, AFM, and spectrofluorometer. Electrochemical experiments were performed with a microcomputer-based electrochemical analyzer. GO, DXR, and GO−DXR were first dispersed in distilled water. The concentrations of DXR and GO in solution of DXR and GO were the same as that in the solution of GO−DXR, respectively. Then 6 μL of the solution was cast on a the surface of a glassy carbon (GC) electrode (diameter = 4 mm). With Ag/AgCl as a reference electrode and platinum electrode as a counter electrode, the electrochemical measurements were carried out in phosphate buffer (50 mM, pH 7.4).

Release of DXR from GO−DXR. The nanohybrids GO−DXR (6 mg) were dispersed in 3 mL of aqueous solution and the dispersion was divided into three equal aliquots. The GO−DXR samples used for the release experiments were placed into the dialysis chambers, which were dialyzed in 60 mL of aqueous solution with pH 2, 7, and 10, respectively. The drug release was assumed to start as soon as the dialysis chambers were placed into the reservoir. The release reservoir was kept under constant stirring, and at various time points, one of the dialysis chambers was taken out for characterization. The concentration of DXR released from GO−DXR into distilled water was quantified using UV spectroscopy.

3. Results and Discussion

On the basis of a recent study,[13,14] GO consists of intact graphitic regions interspersed with sp^3-hybridized carbons containing carboxyl, hydroxyl, and epoxide functional groups on the edge, top, and bottom surfaces of each sheet and sp^2-hybridized carbons on the aromatic network.[15] The large π conjugated structure of GO can form $\pi-\pi$ stacking interaction with the quinone portion of DXR as well as the hydrophobic effect between them. In addition, amino and several hydroxyl groups are also on DXR. The −OH and −COOH groups on the graphene sheet can form a strong hydrogen-bonding interaction with −OH and $-NH_2$ groups in DXR. Their structures are shown in Scheme 1. Therefore, DXR was noncovalently loaded on GO simply by mixing them in aqueous solution with the aid of slight sonication.

The morphology of GO before and after loading with DXR was characterized with AFM in tapping mode, as shown in Figure 1. GO shows a height of 0.8−1.0 nm, suggesting a single layer graphene sheet.[12] The pristine GO shows a smooth surface several hundreds of nanometers in size, as shown in Figure 1A, while many surface protuberances are observed on the surface of GO−DXR nanohybrid, as shown in Figure 1B. Obviously, a large amount of DXR is immobilized onto the GO sheet.

More convincing evidence came from UV−vis spectroscopy (Figure 2). The GO shows a single broad peak at 230 nm, and free DXR solution absorbs strongly at 233, 253, 291, and 480

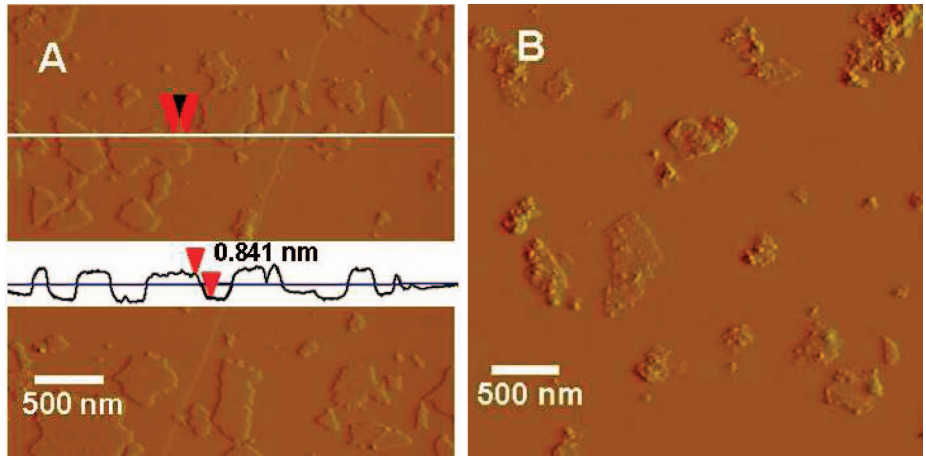

Figure 1. AFM images of GO (A) and GO−DXR (B).

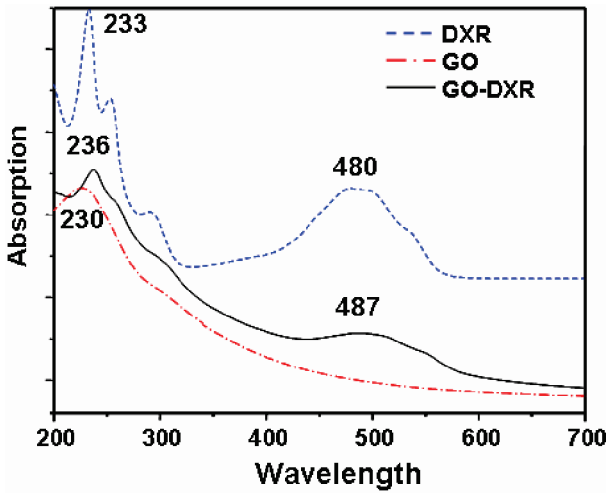

Figure 2. UV visible spectra of DXR, GO, and GO−DXR in aqueous solution.

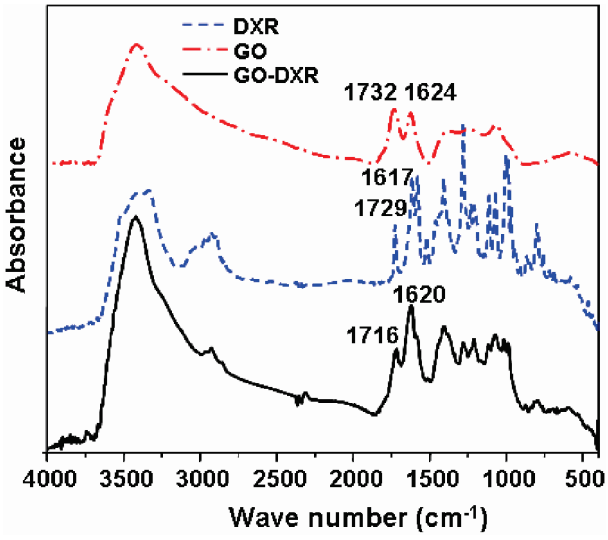

Figure 3. FTIR spectra of DXR, GO, and GO−DXR.

nm. The stacking of DXR onto GO was evident from the spectrum of the GO−DXR nanohybrid solution, which shows the characteristic absorption peaks of DXR clearly. Moreover, after forming the nanohybrid, the absorption peaks of DXR show red-shifts. For example, the peaks of DXR at 233 and 480 nm shifted to 236 and 487 nm after hybridized with GO, which are generally believed due to the ground-state electron donor−acceptor interaction between the two components,[16,17] namely GO and DXR in this study.

The FTIR spectra of GO, DXR, and GO−DXR nanohybrid are shown in Figure 3. The peak at 1732 cm^{-1} corresponding to ν(C═O) in the spectrum of GO and the C═O peak (1729 cm^{-1}) for DXR shift to a lower position at 1716 cm^{-1} after forming GO−DXR nanohybrid. This also indicates that DXR be loaded onto GO, and the shift of characteristic peaks may be due to the hydrogen bonding between these two components. A similar result has been observed for the nanohybrid materials formed by ferrocenecarboxylic acid and single-walled carbon nanotubes.[18]

The loading capacity of DXR on GO was determined by UV spectrum at 233 nm, which was calculated by the difference of DXR concentrations between the original DXR solution and the supernatant solution after loading. The loading of DXR on GO was investigated in different initial DXR concentrations with respect of the same concentration of GO (0.145 mg/mL), as shown in Figure 4a. The loading of DXR on GO is 0.55 mg/mg at the DXR concentration of 0.09 mg/mL. With the increase of the initial DXR concentration, the loading capacity of XDR increases linearly and reaches 2.35 mg/mg at the DXR concentration of 0.47 mg/mL. Much work is needed to investigate the saturated loading capacity of GO toward DXR, even such a value of loading is far beyond the common drug carrier materials, such as carbon nanohorns[19] and polymer vesicles,[20] which is always below 1 mg/mg at saturated carrying concentration. This shows that the graphene is indeed a promising candidate for drug carrier materials. As illustrated in Scheme 1 and Table 1, the interaction between GO and DXR may come from $\pi-\pi$ staking between the conjugated structure of graphene sheet and the quinone portion of DXR and the hydrophobic effect between them mainly. Also, the hydrogen bonding between the −OH and −COOH groups of GO and the −OH and $-NH_2$ groups of DXR may exist. Next we investigated the loading behavior of GO toward DXR at different pH conditions, as shown in Figure 4b.

Figure 4b shows the loading of DXR on GO at the initial DXR concentration of 0.174 mg/mL at pH values of 2, 6, and 10. As expected, the GO shows distinctly different loading capacity toward DXR at different pH values. The loading of DXR on GO is 0.55 mg/mg at pH 2, 0.91 mg/mg at pH 6, and 0.74 mg/mg at pH 10. The highest loading capacity is observed at the neutral condition, rather than acidic or basic conditions. The pH-dependent loading may be due to the different degree of hydrogen-bonding interaction between these two species under different pH conditions. Under neutral condition, four kinds of hydrogen bonding can be formed between −COOH of GO and the −OH of DXR, −COOH of GO and the $-NH_2$ of DXR, −OH of GO and the −OH of DXR, and −OH of GO and the $-NH_2$ of DXR (Table 1). Under acidic conditions, $-NH_2$ of DXR forms $-NH_3^+$ with H^+ and therefore cannot participate in hydrogen bonding. In this case, two kinds of hydrogen bonding can occur between −COOH of GO and the −OH of DXR, and −OH of GO and the −OH of DXR. Furthermore, the H^+ in solution would compete with the hydrogen-bond-forming groups and then weaken the above hydrogen-bonding interaction. Under basic conditions, −COOH of GO exists as $-COO^-$ and cannot form a hydrogen bond with −OH or $-NH_2$ groups of DXR. Two kinds of hydrogen bonding interaction can occur between −OH of GO and the −OH of DXR, and −OH of GO and the $-NH_2$ of DXR. Therefore, the strongest hydrogen-bonding interaction between GO and DXR is expected under neutral conditions, and the highest loading of DXR on GO is obtained. The experimental results indicate that the loading capacity of DXR on GO is larger under basic conditions than that under acidic conditions, which may be due to the stronger hydrogen-bonding interaction under basic conditions than that under acid conditions.

In view of the high loading capacity of GO toward DXR, it may be used as a drug carrier candidate material; herein, the release behavior of DXR from GO is shown in Figure 5. The DXR releases slowly from GO and the release rate gradually declines after 5 h and about only 11% of the total bound DXR was released from the nanohybrid in the first 30 h under neutral conditions (pH 7). As discussed above, the hydrogen-bonding interaction between DXR and GO is the strongest at the neutral condition, resulting in an inefficient release. The release behavior at basic and acidic conditions indicates that the total releasing amount of DXR in the first 30 h for these cases is much higher than at neutral conditions. 25% and 71% of the total bound DXR

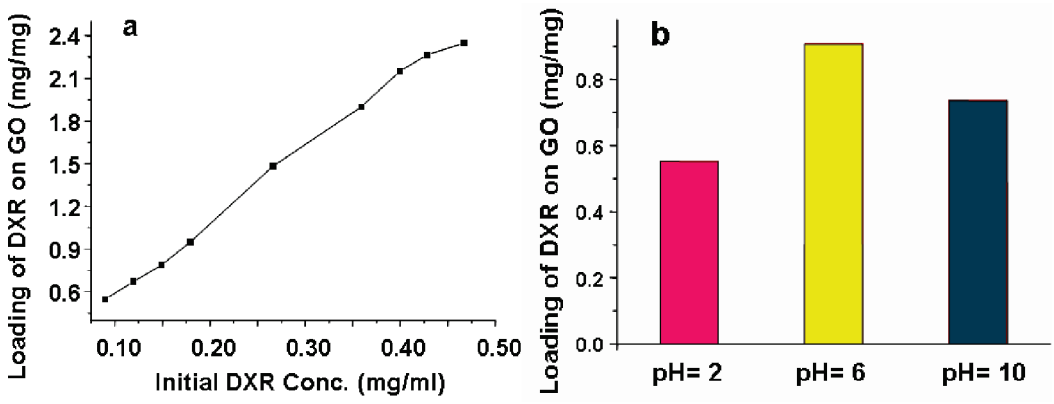

Figure 4. The loading capacity of DXR on GO in different initial DXR concentrations (a) and at different pH values (b).

TABLE 1: Groups That Can Form Hydrogen Bonds in GO and DXR at Different pH Values

pH value	GO	DXR
2	−OH, −COOH	−OH
7	−OH, −COOH	−OH, $-NH_2$
10	−OH	−OH, $-NH_2$

was released from the nanohybrid after 30 h at pH 10 and 2, respectively. Such results may be due to the partial dissociation of hydrogen-bonding interaction under acid and basic conditions, as indicated in the above section. The release amount of DXR from the nanohybrid under acid conditions is much higher than that under basic conditions. Similar to the loading behavior, this may be caused by the stronger hydrogen-bonding interaction under basic conditions than that under acid conditions.

For the interaction between the graphene sheet and DXR, $\pi-\pi$ stacking may be the most important one because the loading of DXR on GO is still high in the case of decreasing of the hydrogen-bonding interactions under acidic conditions. Therefore, the interaction between GO and DXR in the excited-state using fluorescence spectroscopy is illustrated in Figure 6. Free DXR exhibits a fluorescence emission maximum at 593 nm with an excited source at 480 nm. However, upon excitation at the same wavelength, GO−DXR exhibits significant quenching of its emission band. These results imply the presence of a photoinduced electron-transfer process or efficient energy transferring along the GO−DXR interface.[21,22] Similar to the earlier works with daunomycin and single-walled carbon nanotubes,[23] this efficient quenching of fluorescence emission shows that there is strong $\pi-\pi$ stacking interaction between GO and DXR.

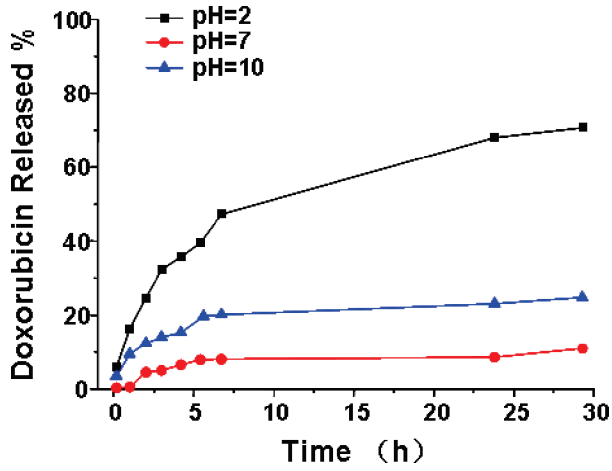

Figure 5. The release of DXR on GO at different pH values.

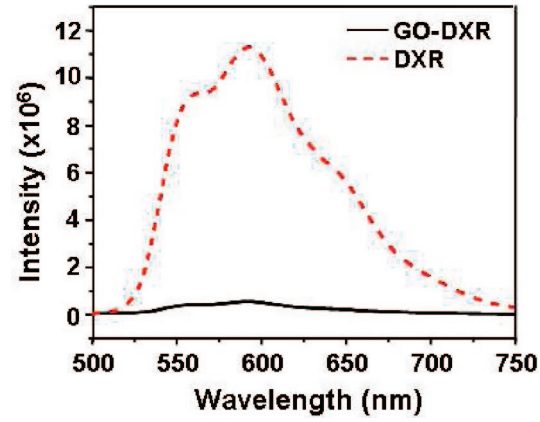

Figure 6. Fluorescence spectra of GO−DXR and DXR in water at the 480 nm excitation wavelength. The concentrations of both GO−DXR and DXR were all controlled to be the same according to the loading of DXR on GO.

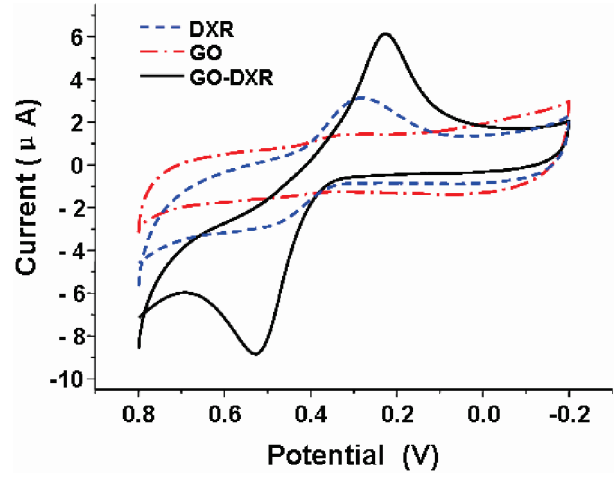

Figure 7. Cyclic voltammetry curves of DXR-, GO-, and GO−DXR-modified GC electrodes at a 50 mV/s scan rate in phosphate buffer (0.05 M, pH 7.4). Both GO and DXR concentrations were controlled to be the same according to the loading of DXR on GO.

Electrochemistry is one of the common tools investigating the electron transfer behavior of nanohybrid of carbon nanotube with electroactive substances. On the basis of the similar chemical structure and physical properties between carbon nanotubes and graphene, cyclic voltametry was used to investigate the electrochemical property of GO−DXR. Figure 7 compares the typical cyclic voltammetry curves using the GO−DXR-modified GC electrode and the control electrodes of GO- and DXR-modified GC electrodes, respectively. The

typical redox couple of peaks of DXR with cathode and anode peak potentials at 0.319 and 0.512 V were observed, which can be attributed to the characteristic peaks of DXR based on the redox reaction of its quinone portion of the molecule.[24] Compared to the redox peak of DXR-modified GC electrode, the redox peak of GO−DXR-modified GC electrode shows significant enhancement at corresponding positions. The enhanced redox reaction current of GO−DXR modified electrode may be attributed to the synergistic effect due to the $\pi-\pi$ stacking between GO and DXR. The interaction between the two components in the homogeneous nanohybrid is efficient in enhancing electron transfer.

4. Conclusions

In this paper, a high loading and pH-dependent release of DXR on GO was investigated. The loading of DXR on GO increased linearly with the increasing of initial DXR concentration as high as 2.35 mg/mg at the initial DXR concentration of 0.47 mg/mL. The pH-dependent loading and releasing may be due to the hydrogen-bonding interactions between GO and DXR. At the same time, the fluorescence spectrum and electrochemical characterization results show that strong $\pi-\pi$ stacking interactions exist between GO and DXR. The highly efficient loading of DXR on GO and excellent electrochemical and photoinduced electron-transfer activity of GO−DXR nanohybrid could thus offer a way to prepare novel GO-based nanohybrids for applications such as drug carriers and biosensors.

Acknowledgment. We gratefully acknowledge the financial support from the NSFC (#20644004, #20774047), MoST (#2006CB932702), and NSF of Tianjin City (#07JCYBJC01700, #07JCYBJC03000, #08JCZDJC25300).

References and Notes

(1) Burger, K. N. J.; Staffhorst, R. W. H. M.; de Vijlder, H. C.; Velinova, M. J.; Bomans, P. H.; Frederik, P. M.; de Kruijff, B. *Nat. Med.* **2002**, *8*, 81.

(2) Matsumoto, A.; Matsukawa, Y.; Suzuki, T.; Yoshino, T.; Kobayashi, M. *J. Controlled Release* **1997**, *48*, 19.

(3) Maeda, H.; Sawa, T.; Kouno, T. *J. Controlled Release* **2001**, *74*, 47.

(4) Seo, S. B.; Yang, J.; Hyung, W.; Cho, E. J.; Lee, T. I.; Song, Y. J.; Yoon, H. G.; Suh, J. S.; Huh, Y. M.; Haam, S. *Nanotechnology* **2007**, *18*, 475105.

(5) Wu, W.; Wieckowski, S.; Pastorin, G.; Benincasa, M.; Klumpp, C.; Briand, J. P.; Gennaro, R.; Prato, M.; Bianco, A. *Angew. Chem., Int. Ed.* **2005**, *44*, 6358.

(6) Murakami, T.; Ajima, K.; Miyawaki, J.; Yudasaka, M.; Iijima, S.; Shiba, K. *Mol. Pharm.* **2004**, *1*, 399.

(7) Liu, Z.; Sun, X.; Nakayama-Ratchford, N.; Dai, H. *ACS Nano* **2007**, *1*, 50.

(8) Geim, A. K.; Novoselov, K. S. *Nat. Mater.* **2007**, *6*, 183.

(9) Zhang, Y. B.; Tan, Y. W.; Stormer, H. L.; Kim, P. *Nature* **2005**, *438*, 201.

(10) Liu, Z.; Robinson, J. T.; Sun, X.; Dai, H. *J. Am. Chem. Soc.* **2008**, *130*, 10876.

(11) Sun, X.; Liu, Z.; Welsher, K.; Robinson, J. T.; Goodwin, A.; Zaric, S.; Dai, H. *Nano Res.* **2008**, *1*, 203.

(12) Becerril, H. A.; Mao, J.; Liu, Z.; Stoltenberg, R. M.; Bao, Z.; Chen, Y. *ACS Nano* **2008**, *2*, 463.

(13) Lerf, A.; He, H. Y.; Forster, M.; Klinowski, J. *J. Phys. Chem. B* **1998**, *102*, 4477.

(14) Hontoria-Lucas, C.; Lopez-Peinado, A. J.; Lopez-Gonzalez, J. DE D.; Rojas-Cervantes, M. L.; Martin-Aranda, R. M. *Carbon* **1995**, *33*, 1585.

(15) OuYang, F.; Huang, B.; Li, Z.; Xiao, J.; Wang, H.; Xu, H. *J. Phys. Chem. C* **2008**, *112*, 12003.

(16) Guldi, D. M.; Marcaccio, M.; Paolucci, D.; Paolucci, F.; Tagmatarchis, N.; Tasis, D.; Vazquez, E.; Prato, M. *Angew. Chem., Int. Ed.* **2003**, *42*, 4206.

(17) Murakami, H.; Nomura, T.; Nakashima, N. *Chem. Phys. Lett.* **2003**, *378*, 481.

(18) Yang, X. Y.; Lu, Y. H.; Ma, Y. F.; Li, Y. J.; Du, F.; Chen, Y. S. *Chem. Phys. Lett.* **2006**, *420*, 416.

(19) Murakami, T.; Ajima, K.; Miyawaki, J.; Yudasaka, M.; Iijima, S.; Shiba, K. *Mol. Pharm.* **2004**, *1*, 399.

(20) Choucair, A.; Soo, P. L.; Eisenberg, A. *Langmuir* **2005**, *21*, 9308.

(21) Guo, Z.; Du, F.; Ren, D. M.; Chen, Y. S.; Zheng, J. Y.; Liu, Z. B.; Tian, J. G. *J. Mater. Chem.* **2006**, *16*, 3021.

(22) Baskaran, D.; Mays, J. W.; Zhang, X. P.; Bratcher, M. S. *J. Am. Chem. Soc.* **2005**, *127*, 6916.

(23) Lu, Y. H.; Yang, X. Y.; Ma, Y. F.; Huang, Y.; Chen, Y. S. *Biotechnol. Lett.* **2008**, *30*, 1031.

(24) Komorsky-Lovric, S. *Bioelectrochemistry* **2006**, *69*, 82.

JP806751K